Vanadium–Iron–Sulfur Clusters Containing the Cubane-type [VFe 3 S 4] Core Unit: Synthesis of a Cluster with the Topology of the P N Cluster of Nitrogenase

ARTICLE *in* INORGANIC CHEMISTRY · AUGUST 2003

Impact Factor: 4.76 · DOI: 10.1021/ic0301369 · Source: PubMed

3 AUTHORS, INCLUDING:

Hong-Cai Zhou
Texas A&M University
235 PUBLICATIONS **19,593** CITATIONS
SEE PROFILE

R. H. Holm
Harvard University
338 PUBLICATIONS **17,425** CITATIONS
SEE PROFILE

Inorg. Chem. **2003**, *42*, 4624–4631

Vanadium–Iron–Sulfur Clusters Containing the Cubane-type $[VFe_3S_4]$ Core Unit: Synthesis of a Cluster with the Topology of the P^N Cluster of Nitrogenase

Jing-Lin Zuo, Hong-Cai Zhou, and R. H. Holm*

Department of Chemistry and Chemical Biology, Harvard University, Cambridge, Massachusetts 02138

Received April 22, 2003

A synthetic method affording a topological analogue of the electron-transfer P-cluster of nitrogenase ($Fe_8S_7(\mu_2\text{-}S_{Cys})_2$) in the P^N state has been devised, based in part on our previous development of cubane-type VFe_3S_4 clusters (Hauser, C.; Bill, E.; Holm, R. H. *Inorg. Chem.* **2002**, *41*, 1615–1624). The cluster $[(Tp)VFe_3S_4Cl_3]^{2-}$ (**1**) is converted to $[(Tp)VFe_3S_4(PR_3)_3]^{1+}$ (R = Et (**2**), Bu (**3**)) by reaction with R_3P. The phosphine ligands are readily substituted, leading to $[(Tp)VFe_3S_4(SR)_3]^{2-}$ (R = Ph (**4**), H (**5**)). Reduction of **2** or **3** with cobaltocene produces the edge-bridged double cubanes $[(Tp)_2V_2Fe_6S_8(PR_3)_4]$ (R = Et (**6**), Bu (**7**)), which are readily converted to $[(Tp)_2V_2Fe_6S_8(SPh)_4]^{4-}$ (**8**). The structures of clusters **3**–**5** and **8** were proven crystallographically. Cluster **8** has the double-cubane structure previously shown for **6**, in which two cubane units are bridged by two Fe–(μ_4-S) bonds. ^{57}Fe isomer shifts are consistent with the formulation $[VFe^{2.33+}{}_3S_4]^{2+}$ for the single cubanes and the all-ferrous description $2[VFe^{2+}{}_3S_4]^{1+}$ for the double cubanes. Reaction of **6** with 4 equiv of $(Et_4N)(HS)$ in acetonitrile results in the insertion of sulfide with concomitant structural rearrangement and the formation of $[(Tp)_2V_2Fe_6S_9(SH)_2]^{4-}$ (**10**), obtained in ca. 50% yield as the Et_4N^+ salt. The cluster has C_2 symmetry, with two all-ferrous VFe_3S_4 fragments bridged by a common μ_6-S atom and two μ_2-S atoms that simulate the bridging atoms in the two Fe–(μ_2-S_{Cys})–Fe bridges of the P^N cluster. The bridge pattern $V_2Fe_6(\mu_2\text{-}S)_2(\mu_3\text{-}S)_6(\mu_6\text{-}S)$ and cluster shape match those of the native cluster. A best-fit superposition of the cores of **10** and the P^N cluster affords a weighted rms deviation in atom positions of 0.33 Å. Cluster **10** and $[(Tp)_2Mo_2Fe_6S_9(SH)_2]^{3-}$, prepared by a related route (Zhang, Y.; Holm, R. H. *J. Am. Chem. Soc.* **2003**, *125*, 3910–3920), demonstrate that the topology of the P^N cluster can be achieved in molecular form in the absence of protein structure (Tp = tris(pyrazolyl)hydroborate).

Introduction

A structural motif of considerable current interest in weak-field M−Fe−S clusters is the edge-bridged double cubane. Here two MFe_3S_4 cubane-type units are bridged by Fe−S interactions to form an Fe_2S_2 rhomb in which the intercubane Fe−(μ_4-S) bond tends to be shorter than the intracubane bond of the same type. The $M_2Fe_6(\mu_3\text{-}S)_6(\mu_4\text{-}S)_2$ core occurs thus far with M atoms transoid in a structure which approaches or achieves centrosymmetry. The structure is illustrated in Figure 1. Clusters are known with M = Fe,[1−3] V,[4] and Mo.[5−9] They approach the core compositions of the crystallographically defined catalytic FeMo-cofactor ($MoFe_7S_9$) and electron-transfer P^N (Fe_8S_9) clusters of nitrogenase.[10−12] For this reason, we have utilized these clusters in synthetic procedures directed toward the biological clusters, which thus far have been achieved only by biosynthesis. The P^N cluster is the more relevant in this investigation and is depicted in Figure

* To whom correspondence should be addressed. E-mail: holm@chemistry.harvard.edu.

(1) Cai, L.; Segal, B. M.; Long, J. R.; Scott, M. J.; Holm, R. H. *J. Am. Chem. Soc.* **1995**, *117*, 8863−8864.
(2) Goh, C.; Segal, B. M.; Huang, J.; Long, J. R.; Holm, R. H. *J. Am. Chem. Soc.* **1996**, *118*, 11844−11853.
(3) Zhou, H.-C.; Holm, R. H. *Inorg. Chem.* **2003**, *42*, 11−21.
(4) Hauser, C.; Bill, E.; Holm, R. H. *Inorg. Chem.* **2002**, *41*, 1615−1624.
(5) Demadis, K. D.; Campana, C. F.; Coucouvanis, D. *J. Am. Chem. Soc.* **1995**, *117*, 7832−7833.
(6) Osterloh, F.; Segal, B. M.; Achim, C.; Holm, R. H. *Inorg. Chem.* **2000**, *39*, 980−989.
(7) Osterloh, F.; Achim, C.; Holm, R. H. *Inorg. Chem.* **2001**, *40*, 224−232.
(8) Han, J.; Koutmos, M.; Al-Ahmad, S.; Coucouvanis, D. *Inorg. Chem.* **2001**, *40*, 5985−5999.
(9) Zhang, Y.; Holm, R. H. *J. Am. Chem. Soc.* **2003**, *125*, 3910−3920.
(10) Peters, J. W.; Stowell, M. H. B.; Soltis, S. M.; Finnegan, M. G.; Johnson, M. K.; Rees, D. C. *Biochemistry* **1997**, *36*, 1181−1187.
(11) Mayer, S. M.; Lawson, D. M.; Gormal, C. A.; Roe, S. M.; Smith, B. E. *J. Mol. Biol.* **1999**, *292*, 871−891.
(12) Einsle, O.; Tezcan, F. A.; Andrade, S.; Schmid, B.; Yoshida, M.; Howard, J. B.; Rees, D. C. *Science* **2002**, *297*, 1696−1700.

10.1021/ic0301369 CCC: $25.00
Published on Web 06/25/2003

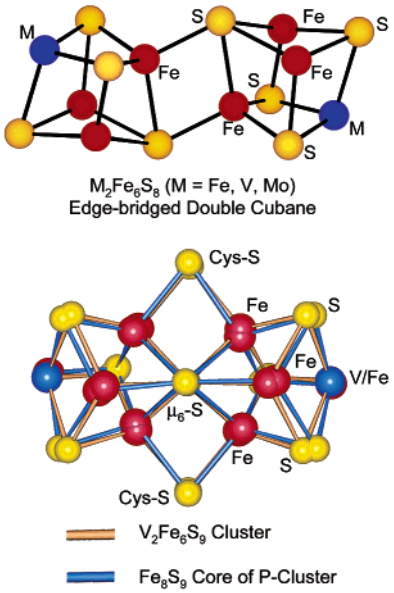

Figure 1. Upper: Structure of the core of an edge-bridged double cubane. Lower: Structure of the core of the P-cluster of nitrogenase in the P^N state. This structure is shown in a best-fit superposition with the $V_2Fe_6S_9$ core of $[(Tp)_2V_2Fe_6S_9(SH)_2]^{4-}$.

1. It contains two distorted cubane units bridged by two μ_2-S_{Cys} atoms and one μ_6-S atom integrated into the bridging pattern $Fe_8(\mu_2\text{-}S)_2(\mu_3\text{-}S)_6(\mu_6\text{-}S)$.

Previous synthetic efforts based on the reaction of the edge-bridged double cubane $[(Cl_4cat)_2(Et_3P)_2Mo_2Fe_6S_8(PEt_3)_4]$[5,6] with hydrosulfide have yielded the clusters $[(Cl_4cat)_6(Et_3P)_6Mo_6Fe_{20}S_{30}]^{8-}$ [13] and $[(Cl_4cat)_4(Et_3P)_4Mo_4Fe_{12}S_{20}K_3(DMF)]^{5-}$.[7] Contained within these complicated structures are two $(Cl_4cat)_2(Et_3P)_2Mo_2Fe_6S_9$ fragments with the same bridging pattern as the P^N cluster and in which two μ_2-S atoms simulate the bridging cysteinates in the latter. A best-fit superposition of the $Mo_2Fe_6S_9$ fragment core with that in *K. pneumoniae* FeMo protein[11] affords a weighted rms deviation of 0.23 Å in atom positions. These results provided the first indication that the P^N cluster topology is synthetically accessible, although not necessarily in an all-iron cluster. However, the properties of the fragments cannot be deconvoluted from those of the entire cluster.

More recently, we have prepared trigonally symmetric MFe_3S_4 single-cubane clusters, rendered in that condition by a tris(pyrazolyl)hydroborate (Tp) ligand at the heterometal site and identical ligands at the iron sites.[4,14] The first such cluster, with M = V, was prepared by Malinak et al.[15] in 1995. These single cubanes have been converted to edge-bridged double cubanes under reducing conditions. They are potential precursors to $M_2Fe_6S_9$ clusters which, if possessing the cofactor or P^N cluster structure, would not have the possibility of geometric isomers. Lower symmetry coordination at the M site can in principle lead to isomers. This approach has been put into practice by the reactions of $[(Tp)_2M_2Fe_6S_8(PEt_3)_4]$ with hydrosulfide to give the clusters $[(Tp)_2M_2Fe_6S_9(SH)_2]^{3-,4-}$ with M = V[16] and Mo.[9,16] We have recently provided a detailed account of the synthesis and certain properties of $[(Tp)_2Mo_2Fe_6S_9(SH)_2]^{3-}$.[9] Here we provide a corresponding report for the analogous vanadium cluster, augmenting our earlier brief account of its synthesis and structure.[16]

Experimental Section

Preparation of Compounds. All operations and manipulations were carried out at room temperature using either Schlenk or standard glovebox techniques. Solvents were dried by distillation from sodium/benzophenone (ether, THF, hexanes) or CaH_2 (acetonitrile) and were thoroughly degassed prior to use. Ether was introduced into solutions by vapor diffusion. Isolated solids were washed with ether and dried in vacuo. Because of the small scale of the preparations, analyses were performed on selected compounds. In ^{1}H NMR spectra, certain pyrazolyl proton signals were not detected; presumably, those nearest the core are broadened by cluster paramagnetism. B−H resonances are broad and in some cases were not located. The spectra of double cubanes $[(Tp)_2V_2Fe_6S_8(PBu_3)_4]$ and $[(Tp)_2V_2Fe_6S_8(SPh)_4]^{4-}$ are complex and would require deuteration or methylation (not carried out) for definitive assignments. However, the identities of all new compounds for which preparations are given were established by X-ray structure determinations (Table 1).

$[(Tp)VFe_3S_4(PBu_3)_3](PF_6)$. $(Me_4N)_2[(Tp)VFe_3S_4Cl_3]\cdot 2MeCN$[4,15] (150 mg, 0.17 mmol) was dissolved in 5 mL of acetonitrile, and PBu_3 (140 mg, 0.69 mmol) was added. After 1 min, $NaPF_6$ (140 mg, 0.83 mmol) in 2 mL of acetonitrile was added. The black reaction mixture was stirred for 16 h, the solvent was removed, and the residue was washed with hexanes. The solid was dissolved in 5 mL of dichloromethane to give a black solution that was filtered through Celite. The filtrate was layered with 15 mL of hexanes, and the mixture was allowed to stand for 2 days. The product was obtained as a black crystalline solid (120 mg, 55%).

$[(Tp)_2V_2Fe_6S_8(PBu_3)_4]$. $[(Tp)VFe_3S_4(PBu_3)_3](PF_6)$ (120 mg, 0.091 mmol) was dissolved in 3 mL of acetonitrile, and a suspension of $[Cp_2Co]$ (30 mg, 0.16 mmol) in 2 mL of acetonitrile was added. The reaction mixture was stirred for 1 min and filtered through Celite. The filtrate was allowed to stand overnight, during which the product separated and was collected as a black crystalline solid (72 mg, 82%). ^{1}H NMR (C_6D_6): δ 1.04, 2.71, 2.84, 6.09, 6.92, 11.7, 16.2, 17.0, 18.5, 22.5.

$(Et_4N)_4[(Tp)_2V_2Fe_6S_8(SPh)_4]$. $[(Tp)_2V_2Fe_6S_8(PEt_3)_4]$ (50 mg, 0.031 mmol) was suspended in 3 mL of acetonitrile, and a solution of $(Et_4N)(SPh)$ (38 mg, 0.16 mmol) in 2 mL of acetonitrile was added. The suspension quickly became a homogeneous black solution. The reaction mixture was stirred for 20 min and filtered through Celite. Slow diffusion of ether into the filtrate afforded the product as a black crystalline solid (54 mg, 83%). ^{1}H NMR (CD_3CN, anion): δ −15.1, −14.4, 5.08, 5.82, 13.5, 20.1, 20.8, 24.4. Anal. Calcd for $C_{74}H_{120}B_2Fe_6N_{16}S_{12}V_2$: C, 42.79; H, 5.82; Fe, 16.13; N, 10.79; S, 18.52; V, 4.90. Found: C, 42.65; H, 5.97; Fe, 16.27; N, 10.71; S, 18.50; V, 4.68.

$(Et_4N)_2[VFe_3S_4(SPh)_3]$. Method A. $[(Tp)VFe_3S_4(PEt_3)_3](PF_6)$[4] (42 mg, 0.04 mmol) was dissolved in 5 mL of acetonitrile, and a solution of $(Et_4N)(SPh)$ (38 mg, 0.16 mmol) in 2 mL of acetonitrile was added. The black solution was stirred overnight and filtered through Celite. Diffusion of ether into the filtrate afforded the

(13) Osterloh, F.; Sanakis, Y.; Staples, R. J.; Münck, E.; Holm, R. H. *Angew. Chem., Int. Ed. Engl.* **1999**, *38*, 2066−2070.
(14) Fomitchev, D. V.; McLauchlan, C. C.; Holm, R. H. *Inorg. Chem.* **2002**, *41*, 958−966.
(15) Malinak, S. M.; Demadis, K. D.; Coucouvanis, D. *J. Am. Chem. Soc.* **1995**, *117*, 3126−3133.
(16) Zhang, Y.; Zuo, J.-L.; Zhou, H.-C.; Holm, R. H. *J. Am. Chem. Soc.* **2002**, *124*, 14292−14293.

Table 1. Crystallographic Data[a]

	[**3**](PF$_6$)	(Et$_4$N)$_2$[**4**]	(Et$_4$N)$_2$[**5**]	[**7**]·CH$_3$CN	(Et$_4$N)$_4$[**8**]·5CH$_3$CN	(Et$_4$N)$_3$[**9**]·CH$_3$CN	(Et$_4$N)$_4$[**10**]·6CH$_3$CN
formula	$C_{45}H_{91}BF_6Fe_3N_6P_4S_4V$	$C_{43}H_{65}BFe_3N_8S_7V$	$C_{25}H_{53}BFe_3N_8S_7V$	$C_{68}H_{131}B_2Fe_6N_{13}P_4S_8V_2$	$C_{84}H_{135}B_2Fe_6N_{21}S_{12}V_2$	$C_{35}H_{76}BFe_3N_{10}S_7V$	$C_{62}H_{120}B_2Fe_6N_{22}S_{11}V_2$
fw, g/mol	1311.66	1147.75	919.47	1969.82	2282.45	1090.78	1985.06
cryst syst	monoclinic	monoclinic	monoclinic	triclinic	monoclinic	triclinic	monoclinic
space group	$P2_1/n$	$C2/c$	$P2_1/n$	$P\bar{1}$	$P2_1/n$	$P\bar{1}$	$I2/a$
a, Å	15.897(15)	45.754(4)	9.4282(9)	13.024(3)	16.4316(18)	12.3508(11)	22.981(7)
b, Å	24.33(2)	11.2589(9)	34.912(3)	14.546(4)	19.725(2)	13.8075(12)	16.858(5)
c, Å	16.750(16)	25.995(2)	11.9207(11)	15.174(4)	16.7771(18)	16.8049(15)	24.753(7)
α, deg	90	90	90	95.991(5)	90	78.638(3)	90
β, deg	98.388(13)	120.709(2)	91.256(2)	112.649(5)	100.236(2)	70.207(2)	96.441(5)
γ, deg	90	90	90	109.443(4)	90	73.718(2)	90
V, Å^3	6401(11)	11513.2(17)	3922.9(6)	2410.6(10)	5351.1(10)	2571.8(4)	9529(5)
Z	4	8	4	1	2	2	4
ρ (calcd), g/cm^3	1.359	1.324	1.557	1.357	1.417	1.409	1.384
2θ range, deg	2.98−50.00	2.08−56.58	3.62−56.60	3.02−56.64	3.20−56.54	2.60−56.60	2.92−45.00
μ, mm^{-1}	1.089	1.188	1.721	1.343	1.241	1.326	1.361
GOF (F^2)	0.934	0.912	1.037	1.060	1.149	0.991	1.246
R_1[b] (wR_2[c])	0.0463 (0.1217)	0.0652 (0.1626)	0.0365 (0.0918)	0.0412 (0.1175)	0.0463 (0.1001)	0.0539 (0.1437)	0.0743 (0.1601)

[a] Data collected at 213 K with graphite monochromatized Mo Kα (λ = 0.71073 Å) radiation. [b] $R_1 = \sum||F_o| - |F_c||/\sum|F_o|$. [c] $wR_2 = \{[w(F_o^2 - F_c^2)^2/w(F_o^2)^2]\}^{1/2}$.

product as black blocklike crystals (40 mg, 88%). ^{1}H NMR (CD$_3$CN, anion): δ −2.27, 5.99, 13.3, 16.4.

Method B. (Et$_4$N)$_4$[(Tp)$_2$V$_2$Fe$_6$S$_8$(SPh)$_4$] (33 mg, 0.016 mmol) and Ph$_3$SbS (5.4 mg, 0.014 mmol) were mixed in 5 mL of acetonitrile. The reaction mixture was stirred for 20 min and filtered through Celite. Diffusion of ether into the filtrate gave black crystals (12 mg, 33%) with a ^{1}H NMR spectrum identical with that of the product of method A.

(Et$_4$N)$_2$[(Tp)VFe$_3$S$_4$(SH)$_3$]. [(Tp)VFe$_3$S$_4$(PEt$_3$)$_3$](PF$_6$) (51 mg, 0.048 mmol) was dissolved in 5 mL of acetonitrile, and a solution of (Et$_4$N)(SH)[17] (25 mg, 0.15 mmol) in 3 mL of acetonitrile was added. The black solution was stirred overnight and filtered through Celite. Vapor diffusion of ether into the filtrate caused separation of the product as black crystals (25 mg, 56%). ^{1}H NMR (CD$_3$CN, anion): δ 5.98, 16.9. Anal. Calcd for $C_{25}H_{53}BFe_3N_8S_7V$: C, 32.66; H, 5.81; Fe, 18.22; N, 12.19; S, 24.41; V, 5.54. Found: C, 32.48; H, 5.83; Fe, 18.32; N, 12.24; S, 24.36; V, 5.38.

(Et$_4$N)$_3$[(Tp)VFe$_3$S$_4$(SH)$_3$]. [(Tp)$_2$V$_2$Fe$_6$S$_8$(PEt$_3$)$_4$]$_2$ (31 mg, 0.019 mmol) was suspended in 3 mL of acetonitrile, and a solution of (Et$_4$N)(HS) (39 mg, 0.24 mmol) in 2 mL of acetonitrile was added. The solid dissolved immediately to give a dark brown solution which was stirred for 2 h and filtered. Slow introduction of ether resulted in the separation of colorless crystals (excess (Et$_4$N)(SH)) and the product as black crystals, which could be mechanically separated and were identified as the title compound by an X-ray structure determination.

(Et$_4$N)$_4$[(Tp)$_2$V$_2$Fe$_6$S$_9$(SH)$_2$]·$^1/_2$CH$_3$CN. [(Tp)$_2$V$_2$Fe$_6$S$_8$(PEt$_3$)$_4$] (52 mg, 0.033 mmol) was suspended in 1 mL of acetonitrile, and a solution of (Et$_4$N)(HS) (22 mg, 0.14 mmol) in 1 mL of acetonitrile was added. The reaction mixture was stirred for 2 h and filtered. The black solid was dissolved in 5 mL of acetonitrile. Slow diffusion of ether into the solution resulted in the separation of the product as a black crystalline solid (27 mg, 48%). ^{1}H NMR (CD$_3$CN, anion): δ 5.61 (2), 6.45 (1), 13.4 (1), 15.1 (2), 16.3 (2). The product analyzed satisfactorily as a hemisolvate. Anal. Calcd for $C_{50}H_{102}B_2Fe_6N_{16}S_{11}V_2$·$^1/_2CH_3$CN: C, 34.82; H, 5.93; Fe, 19.05; N, 13.14; S, 20.05; V, 5.79. Found: C, 34.99; H, 5.84; Fe, 18.36; N, 12.77; S, 20.21; V, 5.97.

Conversion of [(Tp)$_2$V$_2$Fe$_6$S$_9$(SH)$_2$]$^{4-}$ to [(Tp)VFe$_3$S$_4$(SPh)$_3$]$^{2-}$. To a solution of 13.7 mg (0.0078 mmol) of (Et$_4$N)$_4$[(Tp)$_2$V$_2$Fe$_6$S$_9$(SH)$_2$]·$^1/_2$CH$_3$CN in 3 mL of acetonitrile was added a solution of ≳6 equiv of benzenethiol in 1 mL of acetonitrile. The dark brown solution was stirred for 2 h and filtered through Celite. Slow diffusion of ether into the filtrate resulted in the separation of black platelike crystals. X-ray structural analysis and ^{1}H NMR showed that the crystalline product is (Et$_4$N)$_2$[(Tp)VFe$_3$S$_4$(SPh)$_3$] (15.4 mg, 86%).

Chart 1. Designation of Clusters[a]

[(Tp)VFe$_3$S$_4$Cl$_3$]$^{2-}$	**1**[4,15]
[(Tp)VFe$_3$S$_4$(PR$_3$)$_3$]$^{1+}$	R = Et,[4] **2**; Bu, **3**
[(Tp)VFe$_3$S$_4$(SPh)$_3$]$^{2-}$	**4**
[(Tp)VFe$_3$S$_4$(SH)$_3$]$^{2-}$	**5**
[(Tp)$_2$V$_2$Fe$_6$S$_8$(PR$_3$)$_4$]	R = Et,[4] **6**; Bu, **7**
[(Tp)$_2$V$_2$Fe$_6$S$_8$(SPh)$_4$]$^{4-}$	**8**
[(Tp)VFe$_3$S$_4$(SH)$_3$]$^{3-}$	**9**
[(Tp)$_2$V$_2$Fe$_6$S$_9$(SH)$_2$]$^{4-}$	**10**
[(Tp)$_2$Mo$_2$Fe$_6$S$_9$(SH)$_2$]$^{3-}$	**11**[9,16]

[a] Tp = tris(pyrazolyl)hydroborate(1−); Cl$_4$cat = tetrachlorocatecholate(2−). Ligands bound to the heterometal precede V or Mo.

In the sections that follow, clusters are designated numerically as **1**−**11** according to Chart 1.

X-ray Structure Determinations. Structures of the seven compounds in Table 1 were determined. Suitable crystals of [**3**](PF$_6$), (Et$_4$N)$_2$[**4**,**5**], (Et$_4$N)$_4$[**8**]·5MeCN, (Et$_4$N)$_3$[**9**]·MeCN, and (Et$_4$N)$_4$[**10**]·6MeCN were obtained by ether diffusion into acetonitrile solutions. Crystals of [**7**]·MeCN were obtained from the preparative reaction. Crystals were mounted in Infineum oil and placed in a dinitrogen cold stream on a Siemens (Bruker) SMART CCD-based diffractometer or a Bruker-AXS P3 diffractometer equipped with a 1 K CCD area detector. Cell parameters were retrieved with SMART software and refined using SAINT on all observed reflections. Data were collected at 213 K using the following procedure: 606 frames of 0.3° in ω with φ = 0°, 435 frames of 0.3° in ω with φ = 90°, and 235 frames of 0.3° in ω with φ = 180°. An additional 50 frames of 0.3° in ω with φ = 0° were collected to allow for decay corrections. The highly redundant data sets were reduced using SAINT and corrected for Lorentz and polarization effects. Absorption corrections were applied using SADABS supplied by Bruker. Structures were solved by direct methods using SHELX-97. The positions of the metal atoms and

(17) Heller, G.; Eysenbach, W. *Inorg. Chem.* **1979**, *18*, 380−383.

Table 2. Mean Values of Selected Bond Distances (Å) for Single-Cubane Clusters **3**, **4**, **5**, and **9**

		V−N	V−S	Fe−S	V−Fe	Fe−Fe	Fe−P/S
$[(Tp)VFe_3S_4(PBu_3)_3]^{1+}$	**3**	2.175(3)	2.340(2)	2.225(2)	2.703(2)	2.587(2)	2.357(2)
$[(Tp)VFe_3S_4(SPh)_3]^{2-}$	**4**	2.193(5)	2.345(2)	2.271(2)	2.761(1)	2.684(1)	2.289(2)
$[(Tp)VFe_3S_4(SH)_3]^{2-}$	**5**	2.198(2)	2.346(1)	2.276(1)	2.776(1)	2.720(1)	2.297(1)
$[(Tp)VFe_3S_4(SH)_3]^{3-}$	**9**	2.207(3)	2.376(1)	2.304(1)	2.789(1)	2.700(1)	2.345(1)

their first coordination sphere atoms were located from direct-methods *E*-maps; other non-hydrogen atoms were found in alternating Fourier syntheses and least-squares refinement cycles, and during final cycles were refined anisotropically. Hydrogen atoms were placed in calculated positions and refined as riding atoms with a uniform value of U_{iso}. Crystallographic parameters and agreement factors are contained in Table 1.[18]

Other Physical Measurements. All measurements were performed under anaerobic conditions. ^{1}H NMR spectra were determined using a Varian AM-500 spectrometer. Cyclic voltammograms were recorded at 100 mV/s with a Princeton Applied Research model 263 potentiostat/galvanostat using a Pt working electrode and 0.1 M $(Bu_4N)(PF_6)$ supporting electrolyte. Potentials are referenced to the SCE. Mössbauer spectra were collected with a constant acceleration spectrometer. Data were analyzed using WMOSS software (WEB Research Corp., Edina, MN); isomer shifts are referenced to iron metal at room temperature.

Results and Discussion

Synthetic procedures leading to clusters **10** and **11** with $V_2Fe_6S_9$ and $Mo_2Fe_6S_9$ cores, respectively, were developed essentially simultaneously in this laboratory. The method for **10** tends to parallel that for **11** and implicates single- and double-cubane clusters, whose structures were determined crystallographically as a means of identification. Owing to prior detailed structural data and descriptions of these cluster types containing vanadium[4,14,19] or molybdenum,[5−7,9,14,20] metric data presented here are limited to the average bond lengths in Table 2 and bond lengths and angles in Figure 4.

Synthetic Scheme and Intermediates. In this and related work,[9] the goal is the synthesis of *molecular* clusters related in structure to the P^N cluster of nitrogenase. The scheme devised for this purpose is set out in Figure 2; isolated yields are given below. Trigonally symmetric cluster **1** undergoes chloride substitution with tertiary phosphines to afford previously reported **2**[4] and **3** (55%). As for related VFe_3S_4,[4] $MoFe_3S_4$,[9] and Fe_4S_4[3] clusters, the phosphine ligands are quite labile and are readily substituted by thiolate and hydrosulfide to produce clusters **4** (88%) and **5** (56%), respectively. Clusters **1**−**5** are in the $[VFe_3S_4]^{2+}$ oxidation state with an $S = {}^3/_2$ ground state.[4,21] The cubane-type structures of clusters **3** and **4** are shown in Figure 3. Mean bond lengths for **3**−**5** are summarized in Table 2. These reflect the shorter V−Fe and Fe−Fe distances found for phosphine versus thiolate clusters in the same oxidation state.[9] Cluster dimensions are unexceptional. Clusters **4** and **5** exhibit the reversible three-member electron-transfer series 1 in acetonitrile, for which $E_{1/2} = -1.50$, -0.41 V (R = Ph), and -1.56, -0.37 V (R = H), consistent with the behavior of other Tp-ligated $[VFe_3S_4]^{2+}$ clusters.[14] However, phosphine clusters **3** and **4** show at best quasireversible behavior in acetonitrile. Cluster **3**, for example, exhibits a quasireversible step at $E_{1/2} \approx -0.60$ V.

$$[(Tp)VFe_3S_4(SR)_3]^{3-} \rightleftharpoons [(Tp)VFe_3S_4(SR)_3]^{2-} \rightleftharpoons [(Tp)VFe_3S_4(SR)_3]^{1-} \quad (1)$$

However, these clusters are cleanly reduced by cobaltocene in reaction 2 to edge-bridged double cubanes **6**[4] and **7** (82%) with release of phosphine. The formation of a double cubane is doubtless abetted by the lability of the phosphines, which is also manifested by facile substitution with chloride[4] and by thiolate in reaction 3. Cluster **7** is substantially more soluble in dipolar aprotic solvents than is **6**. The double-cubane nature of the reaction products was established by the structures of **7** (metric parameters not included because of their close similarity to **6**[4]) and of **8**, which is presented in Figure 4. The cluster has crystallographically imposed centrosymmetry. It resembles **6** and $[(Tp)_2V_2Fe_6S_8Cl_4]^{4-}$, having transoid vanadium atoms and intercubane Fe−(μ_4-S) bond lengths (Fe3−S5′, 2.273(1) Å) shorter than intracubane bond lengths (Fe3−S5, 2.341(1) Å). Other dimensions are normal.

$$2[(Tp)VFe_3S_4(PR_3)_3]^{1+} + 2Cp_2Co \rightarrow [(Tp)_2V_2Fe_6S_8(PR_3)_4] + 2[Cp_2Co]^{1+} + 2PR_3 \quad (2)$$

$$[(Tp)_2V_2Fe_6S_8(PR_3)_4] + 4PhS^- \rightarrow [(Tp)_2V_2Fe_6S_8(SPh)_4]^{4-} + 4PR_3 \quad (3)$$

Oxidation States. Upon reduction of Fe_4S_4 or MFe_3S_4 clusters, ^{57}Fe isomer shifts increase, signifying increasing ferrous character. Among heterometal cubanes, this behavior is well documented for $MoFe_3S_4$ clusters.[6,14,21,22] For each electron added, the isomer shift increases by ca. 0.1 mm/s, from which it has been concluded that the added electron density is located nearly completely on the Fe_3S_4 core fragment. The latest empirical correlation between isomer shift δ and oxidation state s ($\delta = 1.51-0.42s$ at 4.2 K), based on extensive isomer shift data for synthetic analogues,[23] predicts a $0.42/3 = 0.14$ mm/s change in isomer shift per iron atom in a tetrahedral $FeS_n(SR)_{4-n}$ coordination unit upon one-electron reduction of the Fe_3S_4 fragment. This relation does not take into account whatever small effect a heteroatom

(18) See paragraph at the end of this article for Supporting Information available.
(19) Kovacs, J. A.; Holm, R. H. *Inorg. Chem.* **1987**, *26*, 711−718.
(20) Malinak, S. M.; Coucouvanis, D. *Prog. Inorg. Chem.* **2001**, *49*, 599−662.
(21) Carney, M. J.; Kovacs, J. A.; Zhang, Y.-P.; Papaefthymiou, G. C.; Spartalian, K.; Frankel, R. B.; Holm, R. H. *Inorg. Chem.* **1987**, *26*, 719−724.
(22) Mascharak, P. K.; Papaefthymiou, G. C.; Armstrong, W. H.; Foner, S.; Frankel, R. B.; Holm, R. H. *Inorg. Chem.* **1983**, *22*, 2851−2858.

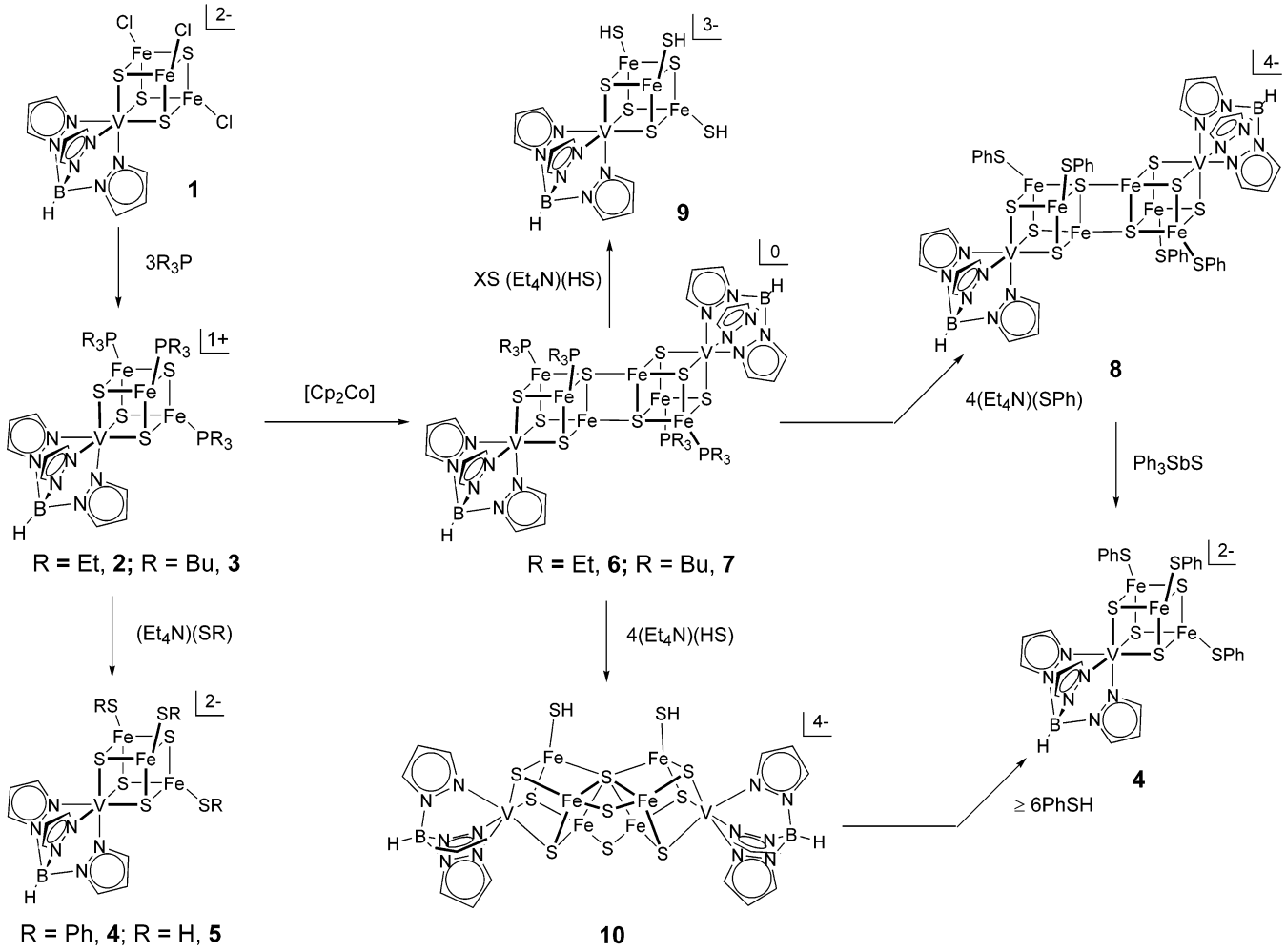

Figure 2. Synthetic scheme affording monocubane clusters **2**−**5** and **9**, edge-bridged double cubanes **6**−**8**, and cluster **10** with P^N-cluster topology.

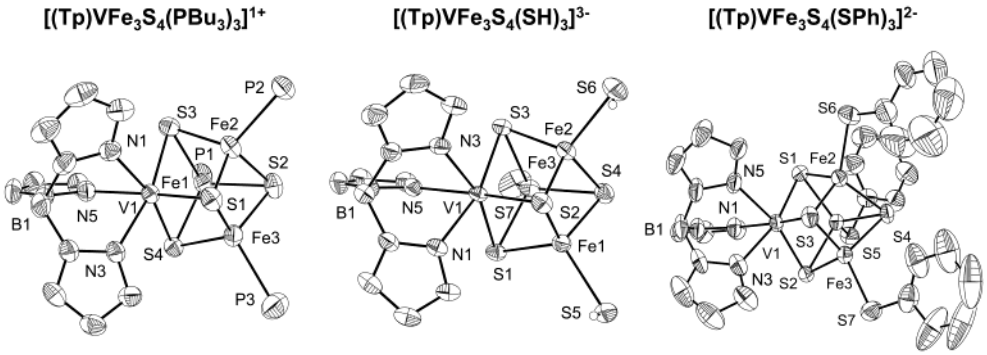

Figure 3. Structures of $[(Tp)VFe_3S_4(PBu_3)]^{1+}$ (**3**), $[(Tp)VFe_3S_4(SH)_3]^{3-}$ (**9**), and $[(Tp)VFe_3S_4(SPh)_3]^{2-}$ (**4**), showing 50% probability ellipsoids and partial atom labeling schemes. The alkyl groups in **3** have been omitted for clarity.

may have on the intrinsic isomer shift of a neighboring atom. While data are less extensive for VFe_3S_4 clusters, the behavior is quite similar. Elsewhere, we have argued that the 0.12 mm/s difference between the isomer shifts of $[(Tp)VFe_3S_4Cl_3]^{1-}$ and **1** indicates fragment reduction and a $[V^{3+}Fe^{2.33+}{}_3S_4]^{2+}$ core formulation.[4] Assembled in Table 3 are isomer shift data for VFe_3S_4 clusters in the three oxidation states known for isolated clusters. These are the states included in electron transfer series 1. The previously observed terminal ligand trend in (mean) isomer shift, $\delta = Cl^- > RS^- > R_3P$, is evident. In chloride clusters, the isomer shift difference between **1** and $[(Tp)_2V_2Fe_6S_8Cl_4]^{4-}$ is 0.09 mm/s and between phosphine clusters **2** and **6**/**7** is 0.12−0.13 mm/s.

From the empirical relationship, $s = 2.2$ for thiolate cluster **8**. With these results, we conclude that double cubanes **6**-**8** are best formulated as $[V^{3+}Fe^{2+}{}_3S_4]^{1+}$.

Topological P^N Cluster. Reaction of double cubane **6** with 4 equiv of hydrosulfide in reaction 4 in acetonitrile affords cluster **10**, obtained as the Et_4N^+ salt hexasolvate in 48%

(23) Venkateswara Rao, P.; Holm, R. H., *Chem. Rev.*, submitted for publication.

$[(Tp)_2V_2Fe_6S_8(SPh)_4]^{4-}$

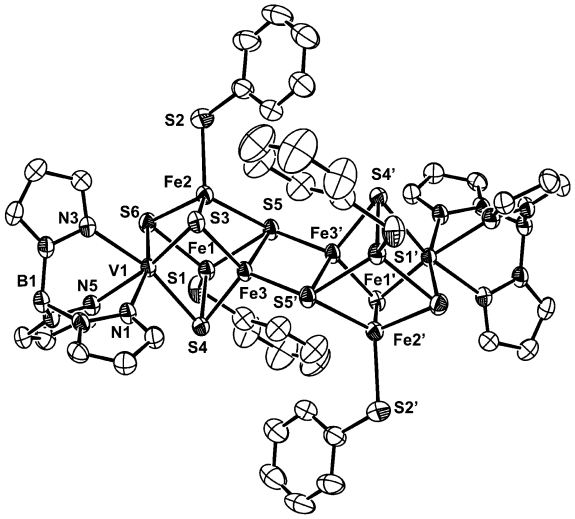

Figure 4. Structure of edge-bridge double cubane $[(Tp)_2V_2Fe_6S_8(SPh)_4]^{4-}$, showing 50% probably ellipsoids and a partial atom labeling scheme. Primed and unprimed atoms are related by crystallographically imposed centrosymmetry. Selected bond distances (Å) and angles (deg): V−N, 2.211(2); V−S, 2.367(1); V−Fe, 2.761(1); Fe−Fe, 2.695 (mean of 3); Fe−S, 2.262(1) (mean of 6 for S3, S4, and S6); Fe1−S5, 2.361(1); Fe2−S5, 2.347(1); Fe3−S5, 2.341(1); Fe3′−S5, 2.273(1); Fe3−Fe3′, 2.678(1); Fe1−S1, 2.327(1); Fe2−S2, 2.314(1); Fe3−S5−Fe3′, 70.93(3); S5−Fe−S5′, 109.07(3).

Table 3. Zero-Field Mössbauer Parameters of VFe_3S_4 Clusters[a]

	δ[b] (mm/s)	ΔE_Q[b] (mm/s)	ref
	$[VFe_3S_4]^{3+}$		
$[(Tp)VFe_3S_4Cl_3]^{1-}$	0.43	1.17	4
	$[VFe_3S_4]^{2+}$		
$[(Tp)VFe_3S_4Cl_3]^{2-}$ [c] (**1**)	0.65 (1), 0.50 (2)	1.15 (1), 1.10 (2)	4
$[(Tp)VFe_3S_4(PEt_3)_3]^{1+}$ [c] (**2**)	0.38	1.02	4
	$[VFe_3S_4]^{1+}$		
$[(Tp)_2V_2Fe_6S_8Cl_4]^{4-}$	0.64	0.83	4, *d*
$[(Tp)_2V_2Fe_6S_8(PEt_3)_4]$ (**6**)	0.49 (1), 0.51 (2)	1.32 (1), 0.90 (2)	4
$[(Tp)_2V_2Fe_6S_8(PBu_3)_4]$ (**7**)	0.49 (1), 0.52 (2)	1.61 (1), 0.96 (2)	*d*
$[(Tp)_2V_2Fe_6S_8(SPh)_4]^{4-}$ (**8**)	0.60 (1), 0.56 (2)	0.73 (1), 0.96 (2)	*d*
$[(Tp)_2V_2Fe_6S_9(SH)_2]^{4-}$ (**10**)	0.52 (2), 0.59 (1)	1.23 (2), 0.65 (1)	*d*
$[(Tp)_2Mo_2Fe_6S_9(SH)_2]^{3-}$ (**11**)	0.55	0.62[e]	9,16

[a] Data at 4.2 K unless otherwise indicated. [b] Relative intensities of quadrupole doublets in parentheses. [c] 80 K. [d] This work. [e] Broadened quadrupole doublet.

yield. Previously, we reported isolation of the hexasolvate in 70% yield by ether diffusion into an acetonitrile solution for the purpose of obtaining single crystals.[16] Repetitions of the bulk preparation described here consistently gave yields near 50%. The compound is obtained as a black air-sensitive crystalline solid. Reaction 4 results in the insertion of a sulfide atom into the $[V_2Fe_6S_8]^{2+}$ core of **6** without change in oxidation state (vide infra). The structure of the cluster is presented in two views in Figure 5. Selected metric parameters are collected in Table 4.

$$[(Tp)_2V_2Fe_6S_8(PEt_3)_4] + 4HS^- \rightarrow [(Tp)_2V_2Fe_6S_9(SH)_2]^{4-} + H_2S + 4PEt_3 \quad (4)$$

Cluster **10** is isostructural with its molybdenum analogue **11**,[9,16] which is nearly isoelectronic (112 vs 113 valence electrons). The cluster has a crystallographically imposed

$[(Tp)_2V_2Fe_6S_9(SH)_2]^{4-}$

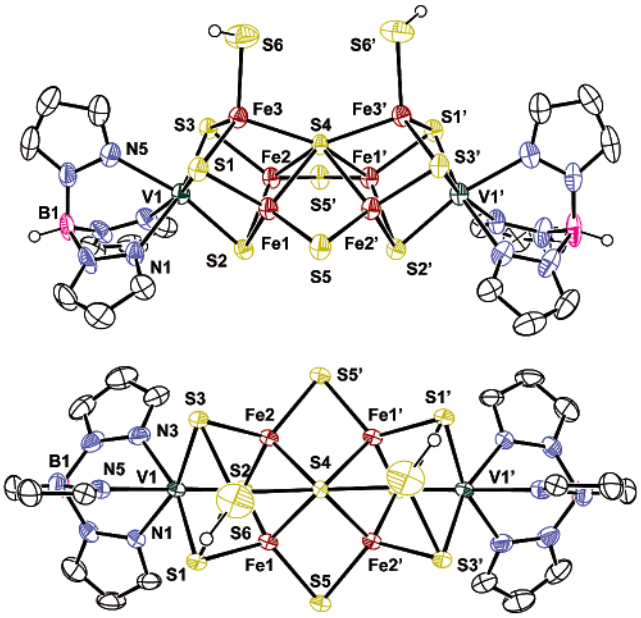

Figure 5. Structure of $[(Tp)_2V_2Fe_6S_8(SPh)_4]^{4-}$ displayed with a side view (upper) and a top view (lower) and showing 50% probability ellipsoids and a partial atom labeling scheme. Primed and unprimed atoms are related by a crystallographic twofold axis.

Table 4. Selected Bond Distances (Å) and Angles (deg) for $[(Tp)_2V_2Fe_6S_9(SH)_2]^{4-}$

V1−N1	2.213(6)	V1−N3	2.210(7)
V1−N5	2.226(7)	V1−S1	2.374(2)
V1−S2	2.373(2)	V1−S3	2.372(2)
V1−Fe1	2.833(2)	V1−Fe2	2.833(2)
V1−Fe3	2.754(2)	Fe1−S1	2.274(2)
Fe1−S2	2.288(2)	Fe1−S4	2.420(2)
Fe1−S5	2.244(2)	Fe1−Fe3	2.694(2)
Fe1−Fe2	2.783(2)	Fe2−Fe3	2.764(2)
Fe1−Fe2′	2.778(2)	Fe2−S3	2.274(2)
Fe2−S2	2.292(2)	Fe2−S4	2.401(2)
Fe2−S5′	2.238(2)	Fe3−S3	2.276(2)
Fe3−S1	2.266(2)	Fe3−S4	2.372(2)
Fe3−S6	2.327(3)		
Fe1−S5−Fe2′	76.59(7)	Fe1−S4−Fe2	70.51(6)
Fe1−S4−Fe3	68.40(4)	Fe1−S4−Fe1′	109.6(1)
Fe1−S4−Fe2′	70.36(6)	Fe1−S4−Fe3′	138.99(6)
Fe2−S4−Fe3	70.79(4)	Fe2−S4−Fe2′	109.0(1)
Fe3−S4−Fe3′	140.8(1)	Fe3−S4−Fe2′	135.92(5)

twofold axis which contains atom S4 and is perpendicular to the plane Fe(1,1′)Fe(2,2′). Comparison with Figure 1 immediately reveals that **10** possesses the topology of the P^N cluster of nitrogenase. The core bridging arrangement is $[V_2Fe_6(\mu_2\text{-}S)_2(\mu_3\text{-}S)_6(\mu_6\text{-}S)]^0$. Each iron has distorted tetrahedral coordination. Atoms Fe(1,2) are coordinated entirely by sulfide, while atom Fe3 has a terminal hydrosulfide ligand. Two cubane-type VFe_3S_4 species are bridged through an uncommon μ_6-S4 atom, the most conspicuous feature of the structure, and by μ_2-S(5,5′), which simulate cysteinate bridges in the native cluster. The $(Tp)VFe_3S_3$ cuboidal fragments of precursor **6** are evident in **10**, although we do not know if they remained intact during reaction 4. In the conversion of **6** to **10**, several large structural changes occur. The bridge rhomb $Fe_2(\mu_4\text{-}S)_2$ is disrupted, two Fe−(μ_2-S)−Fe bridges are formed, and six Fe−(μ_6-S)−Fe bridges are created

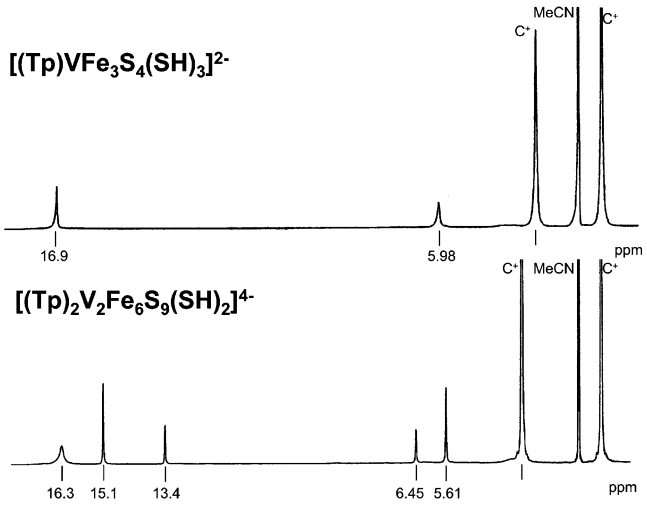

Figure 6. ^{1}H NMR spectra of $[(Tp)VFe_3S_4(SH)_3]^{2-}$ (upper) and $[(Tp)_2V_2Fe_6S_9(SH)_2]^{4-}$ in CD_3CN solutions at 25 °C (C^+ = cation).

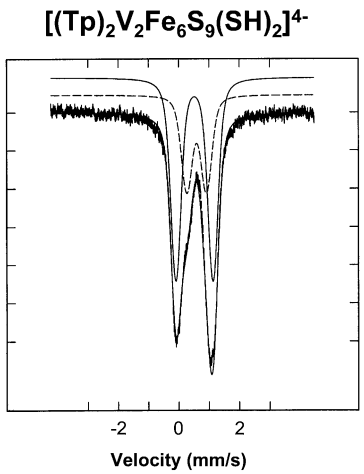

Figure 7. Mossbauer spectrum of $[(Tp)_2V_2Fe_6S_9(SH)_2]^{4-}$ as the polycrystalline Et_4N^+ salt at 4.2 K. The spectrum fitted with two quadrupole doublets using the parameters in Table 3.

involving atoms on the Fe_3 faces of the two cuboidal fragments. Bond lengths follow the usual order Fe−(μ_2-S) (2.241(2) Å) < Fe−(μ_3-S) (2.278(3) Å) < Fe(μ_6-S) (2.40(2) Å); mean values are indicated. Other dimensions are unexceptional. Additional structural features described in the more detailed treatment of cluster **11**[9] apply to **10** with slight changes in bond angles and distances; these are not repeated here. The structure of **10** is maintained in solution. The ^{1}H NMR spectra of trigonally symmetric **5** and **10** are compared in Figure 6, which clearly demonstrates the 2:1 inequivalence of pyrazolyl rings required by the C_2 symmetry of the latter. (One pyrazolyl resonance was not located for each cluster.)

The Mössbauer spectrum of cluster **10**, shown in Figure 7, consists of two quadrupole doublets fitted in a 2:1 intensity ratio. Given the symmetry of the cluster, we associate the smaller doublet with atoms Fe(3,3′) carrying terminal hydrosulfide ligands. The individual coordination units are all very similar. The empirical relationship with $\delta_{av} = 0.54$ mm/s gives $s = 2.3$. Further, the Fe−SH bond length of 2.327(3) Å is essentially the same as that in all-ferrous **9** (2.345(1) Å) and longer than the distance in **5** (2.297(1) Å). Consequently, we describe the core of **10** by the all-ferrous formulation $[V^{3+}{}_2Fe^{2+}{}_6S_9]^0$; i.e., the conversion **6** → **10** is not a redox process. When **6** was treated with excess (12 equiv) of $(Et_4N)(HS)$ in acetonitrile, $(Et_4N)_3$[**9**] was isolated and identified by an X-ray structure determination (Table 2, Figure 3). Attempts to achieve the $[V_2Fe_6S_9]$ core by reaction of **8** with 1 equiv of Ph_3SbS and accompanying reduction of sulfur to sulfide by two thiolate ligands resulted instead in oxidative cleavage to **4** in low yield (33%).

Relation of the Synthesis of $[(Tp)_2Mo_2Fe_6S_9(SH)_2]^{3-}$. Cluster **11** has been synthesized by a reaction sequence similar to that of Figure 2.[9] In the final reaction, it was found that 3 equiv of hydrosulfide are optimal, affording $(Et_4N)_3$[**11**]·2MeCN in high yield (86%). We interpret this result in terms of reactions 5 and 6, leading to overall reaction 7. Under this scheme, the fully reduced cluster reduces H_2S formed in the first step and becomes oxidized to **11** in the second step. (There being no evident alternative in a stoichiometric reaction, dihydrogen is invoked as the reduction product.) In reaction 4, cluster **10**, with its highly reduced core, might be expected to react similarly with H_2S. However, we have not detected $[(Tp)_2V_2Fe_6S_9(SH)_2]^{3-}$; voltammetry of **10** in acetonitrile results in at least three irreversible oxidations at −1.4 to 0 V.

Possibly the cluster does react with H_2S to afford species removed in workup, which could account for the smaller yield of ca. 50%. Using a more easily quantitated protic substrate, **10** was found to reduce benzenethiol in the two-electron reduction reaction 8. With ≳6 equiv of benzenethiol, $(Et_4N)_2$[**4**] (86%) is obtained. The same cluster is formed in reduced yield with 2 equiv of thiol. Elsewhere we have shown that **11** undergoes a similar cluster cleavage reaction with 6 equiv of thiol.[9] These results may be another manifestation of a behavior we have encountered repeatedly, viz., the cluster stability order $MoFe_3S_4 \gg VFe_3S_4$ for clusters with the same or similar ligand environments and differing by one or more valence electrons.

$$[(Tp)_2Mo_2Fe_6S_8(PEt_3)_4] + 4HS^- \rightarrow [(Tp)_2Mo_2Fe_6S_9(SH)_2]^{4-} + H_2S + 4PEt_3 \quad (5)$$

$$[(Tp)_2Mo_2Fe_6S_9(SH)_2]^{4-} + H_2S \rightarrow [(Tp)_2Mo_2Fe_6S_9(SH)_2]^{3-} + HS^- + {}^1/_2H_2 \quad (6)$$

$$[(Tp)_2Mo_2Fe_6S_8(PEt_3)_4] + 3HS^- \rightarrow [(Tp)_2Mo_2Fe_6S_9(SH)_2]^{3-} + 4PEt_3 + {}^1/_2H_2 \quad (7)$$

$$[(Tp)_2V_2Fe_6S_9(SH)_2]^{4-} + 6PhSH \rightarrow 2[(Tp)VFe_3S_4(SPh)_3]^{2-} + 3H_2S + H_2 \quad (8)$$

In addition to core bridging patterns, clusters **10** and **11** have the same overall shape as does the P^N cluster. A best-fit superposition of the $V_2Fe_6S_9$ core of **10** with the core atoms of the native cluster (Figure 1) leads to a weighted rms deviation of 0.33 Å in atom positions. The corresponding deviation for **11** is 0.38 Å.[9] These results confirm that the topology of the P^N cluster can be achieved in molecular form in the absence of protein structure. The next objective is to

achieve an all-iron cluster with this topology, possibly through rearrangments of $Fe_8S_8^3$ or other high-nuclearity clusters. In this context, we note the very recent synthesis of the cluster $[Fe_8S_7(N(SiMe_3)_2)_4(SC(NMe_2)_2)_2]$, whose Fe_8S_7 portion has the P^N-cluster topology, in a self-assembly system.[24] This procedure bears no obvious resemblance to that implemented here.

Acknowledgment. This research was supported by research grant NIH GM 28856. We thank Drs. Y. Zhang and P. Venkateswara Rao for useful discussions and experimental assistance.

(24) Ohki, Y.; Sunada, Y.; Honda, M.; Katada, M.; Tatsumi, K. *J. Am. Chem. Soc.* **2003**, *125*, 4052−4053.

Note Added after ASAP: Due to a production error, the version of this paper posted ASAP on June 25, 2003, contained an error in the Figure 6 caption. The caption is correct in the version posted on July 2, 2003.

Supporting Information Available: X-ray crystallographic files in CIF format for the structure determinations of the seven compounds in Table 1. This material is available free of charge via the Internet at http://pubs.acs.org.

IC0301369